Chaotic Modeling and Simulation (CMSIM) **1: 27-39, 2015**

Transient Processes in a Model Multilayer Nanosystem with Nonlinear Fractal Oscillator

Valeriy S. Abramov

Donetsk Institute for Physics and Engineering named after A.A. Galkin,
National Academy of Sciences of Ukraine
E-mail: vsabramov@mail.ru

Abstract: Within the framework of the two-point model the states of deformation and stress fields of a fractal quantum dot, the stochastic state of discrete lattice in a model multilayer nanosystem are investigated. This uses the theory of fractional calculus and the concept of fractal. Accounting for the effect of bifurcation of solutions of nonlinear equations leads to the appearance of four branches of the lattice nodes displacement function. The numerical modelling of the complex deformation field behaviour is fulfilled on a rectangular discrete lattice. It is shown that for inverse (with a negative fractal index) states of nonlinear fractal oscillator there is an interval of change of this index with anomalous behaviour of the deformation field: there is no effective attenuation within the interval. The possibility of appearance of different transition effects such as induction, avalanches, supernutation, echo in the model multilayer nanosystem with nonlinear fractal oscillator is shown.
Keywords: fractal quantum dot, stochastic state of discrete lattice, deformation and stress fields, inverse states of fractal oscillator, model multilayer nanosystem.

1. Introduction

The actuality of fundamental research of individual quantum systems [1-9] is related to the possible use of them in quantum information technology [2-4]. As the information carrier (units, bits) the quanta of light – photons [1] are used. The recording and subsequent reading of quantum information (encoded in the polarization states of photons) are carried out on quantum states of single atoms or collective quantum states of the atomic ensemble. In the theoretical model description the main object is a qubit – two-level quantum system [5]. In the study of spontaneous parametric scattering, correlations and entanglement in quantum states of the system other model objects of types qutrit and ququarts [6] – the number of quantum systems with more than two levels – have been used. The quanta of vibrational excitations of the lattice – phonons, fractons [7] – can be used as another media. There are various mechanisms of relations and mutual transformations of some information carriers (photons) into others (phonons) in active nanostructured elements of quantum systems [8]. In [2] the behavior of the Fermi gas of ultracool atoms ^{40}K, trapped in an optical trap is studied. The existence of Dirac points when changing the lattice anisotropy and minimum energy gap within the Brillouin zone is shown. In [3] the Dirac fermions and topological phase in molecular graphene are studied. Near singular points Dirac fermions in molecular graphene show quantum and statistical

Received: 19 July 2014 / Accepted: 12 December 2014

ISSN 2241-0503

features of behavior. In [9] the interaction of a single localized electron with Bose-Einstein condensate has been studied. It was shown that this electron can excite phonons and collective oscillations of all condensation. Individual quantum systems are also intensively studied on the base of organic semiconductors for the purpose of their application in quantum electronics, optics, spin information technology (spintronics). So, in [4] by the spin echo method the system of spin quantum qubits based on copper (CuP_c – cupper phthalocyanine) in organic films is studied. Physical properties of the arising transient processes of a spin type induction, echo were studied. Physical properties of these quantum systems (nanosystems) are essentially nonlinear. The methods of nonlinear dynamics have been applied to the theoretical description of the chaos [10] in structural mechanics [11], the analysis of nonlinear chaotic models [12], rare attractors and nonlinear oscillators [13]. In [14] it is proposed to use fractal nanotraps to capture individual particles or groups of particles in order to study their physical properties. At the same time it becomes necessary to conduct experimental and theoretical study of the properties of fractal quasi-two-dimensional and volumetric structures in the model multilayer nanosystems. In [14-20], the models of fractal dislocation [15-18] and fractal quasi-two-dimensional structures were considered as active elements in nanosystems [19]. In order to describe possible correlation effects and statistical properties of the deformation field of fractal dislocation a two-point model was proposed [18]. At excess of critical parameter values there are possible effects of bifurcation [17] solutions – the appearance of several branches in the energy spectrum. From the analysis of the behavior of the correlation functions of the first and second order on the dimensionless time the possibility of transition effects such as induction, avalanches, self-induced transparency, echo, effects of supernutation and propagation of linear fractal dislocation is shown [8].

The aim of this article is to study the deformation fields (after the bifurcation of solutions) of the fractal quantum dot, stochastic discrete lattice state, transient processes in model multilayer nanosystem with nonlinear fractal oscillator.

2. Nonlinear fractal oscillator in nanosystem

At construction of model of fractal dislocation in the [14-20] the Hamilton operator $\hat{H}_2$ from [15, 20] was used for the energy spectrum of fractal dislocation

$$\hat{H}_2 = \varepsilon_1\hat{n}_1 + \varepsilon_2\hat{n}_2 + \varepsilon_3\hat{n}_3';\ \hat{n}_1 = \hat{a}_1^+\hat{a}_1;\ \hat{n}_2 = \hat{a}_2^+\hat{a}_2;\quad \hat{n}_3' = \hat{a}_3\hat{a}_{\mathbf{3}}^+;\ \hat{n}_3 = \hat{a}_{\mathbf{3}}^+\hat{a}_3. \quad (1)$$

$$\hat{H}_2 = \hat{H}_1 + b_0\hat{b}_{\alpha 3};\quad \hat{H}_1 = \varepsilon_2(\hat{n}_1 + \hat{n}_2) + \varepsilon_3\hat{n}_3.$$

Here $\hat{n}_1, \hat{n}_2, \hat{n}_3$ are the operators of occupation numbers of states of dislocation with non-dimensional own energies $\varepsilon_1 = \varepsilon_2, \varepsilon_3$. The relations between the new $\hat{a}_1^+, \hat{a}_2^+, \hat{a}_3$ and old $\hat{\psi}_1, \hat{c}^+, \hat{c}$ operators are defined by expressions

$$\hat{a}_1^+ = t_{11}\hat{\psi}_1 + t_{21}\hat{c}^+ + t_{31}\hat{c};\ \hat{a}_2^+ = t_{12}\hat{\psi}_1 + t_{22}\hat{c}^+ + t_{32}\hat{c};\ \hat{a}_3 = t_{23}\hat{c}^+ + t_{33}\hat{c};\ \hat{\psi}_1 = D_z^{\alpha}. \quad (2)$$

In expressions (2) the elements t_{ij} of the matrix $\hat{T}$ are defined by the relations

$$t_{11} = k';\quad t_{12} = -k;\quad t_{13} = 0;\quad t_{21} = k\,cn(u_\alpha, k);\quad t_{22} = k'\,cn(u_\alpha, k);$$

$t_{23} = -sn(u_\alpha, k)$; $t_{31} = k\,sn(u_\alpha, k)$; $t_{32} = k'sn(u_\alpha, k)$; $t_{33} = cn(u_\alpha, k)$. (3)

Here k and $u_\alpha = F(\varphi_\alpha, k)$ are the module and the argument of the Jacobi elliptic functions $sn(u_\alpha, k)$, $cn(u_\alpha, k)$; $(k')^2 = 1 - k^2$; F is an incomplete elliptic integral of the first kind; φ_α is the polar angle. Using (2), we find the commutation relations for the new operators

$$[\hat{a}_3, \hat{a}_3^+] = \hat{n}_3' - \hat{n}_3 = b_0 \hat{b}_{\alpha 3} \;;\; b_0 = 1 - 2n_{30} \;;\; n_{30} = sn^2(u_\alpha, k);$$

$$\hat{b}_{\alpha 3} = [\hat{\psi}_2, \hat{z}] = (1-\alpha) I_z^\alpha = [\hat{c}, \hat{c}^+] \;;\; \hat{\psi}_2 = D_z^{1-\alpha} \;;\; \hat{b}_{\alpha 2} = [\hat{\psi}_1, \hat{z}] = \alpha I_z^{1-\alpha}, \quad (4)$$

where $\hat{z}$ is the coordinate operator. The structure of operators of fractional partial derivative (integral) of the Riemann-Liouville D_z^α (I_z^α) on dimensionless coordinate z with the index order α is defined as

$$D_z^\alpha \Phi = \partial_z \int_{z_0}^z \Phi(\xi) |z - \xi|^{-\alpha} \, d\xi / \Gamma(1-\alpha), \quad I_z^\alpha \Phi = \int_{z_0}^z \Phi(\xi) |z - \xi|^{\alpha - 1} \, d\xi / \Gamma(\alpha), \quad (5)$$

where ∂_z is the operator of ordinary partial derivative on z; Γ is gamma function. Indices $\alpha, 1-\alpha$ have the meaning of fractal dimensions along the axis Oz. Acting by the operator $\{\hat{c}, \hat{c}^+\} = \hat{c}\hat{c}^+ + \hat{c}^+\hat{c} = \hat{z}^2 - \hat{\psi}_2^2$ to the function $\Phi_{\alpha c}$, we obtain the equation a fractal oscillator

$$(\hat{z}^2 - \hat{\psi}_2^2)\Phi_{\alpha c} = (\hat{z}^2 - D_z^{1-\alpha} D_z^{1-\alpha})\Phi_{\alpha c} = (\hat{c}\hat{c}^+ + \hat{c}^+\hat{c})\Phi_{\alpha c} = (2n_{\alpha c} + 1)\Phi_{\alpha c}. \quad (6)$$

Here $n_{\alpha c}$, $\Phi_{\alpha c}$ are the eigenvalues (generally fractional values, may depend on z, α), eigenfunctions of the fractal oscillator. Acting by the operator $D_z^\alpha \hat{b}_{\alpha 3}$ on the left to the function $\Phi_{\alpha c}$, we obtain the nonlinear equation

$$D_z^\alpha \hat{b}_{\alpha 3} \Phi_{\alpha c} = D_z^\alpha [\hat{c}, \hat{c}^+] \Phi_{\alpha c} = (1-\alpha)\Phi_{\alpha c}. \quad (7)$$

To find the eigenvalues $n_{\alpha c}$ and eigenfunctions $\Phi_{\alpha c}$ the equations (6), (7) must be solved together. These equations are fundamental to describe the nonlinear fractional oscillator. Dimensionless displacement u of points of fractal dislocation (deformation field) is connected with a parameter λ_α (stress field) by model relations (Hooke's law) $u = \lambda_\alpha / \lambda_0 = F(\varphi, k)$, $u_\alpha = u - u_0$, where λ_0 is the normalization parameter; u_0 is the constant (critical) displacement.

In this two-point model [18] based on the Hamiltonian $\hat{H}_2$ (1) the deformation fields of the stochastic discrete lattice state, the fractal quantum dot in a model sample of finite nanosize with volumetric discrete lattice $N_1 \times N_2 \times N_3$ is investigated. The deviations of the lattice nodes from the state of equilibrium in a separate plane $N_1 \times N_2$ for two different points of $z_1(j, j_z)$ and $z_2(j, j_z)$ are described by non-hermitian displacements operators $\hat{u}(z_1)$ and $\hat{u}(z_2)$, corresponding to the rectangular matrix with dimensions $N_1 \times N_2$, $j \in [1, N_3]$.

The value of j_z plays the role of dimensionless current discrete time [8, 20]. The original rectangular matrix displacement $\hat{u}(z_1)$ and $\hat{u}(z_2)$ with elements $u_{nm}(z_1) = u_{\varepsilon s}(z_1)$, $u_{nm}(z_2) = u_{\varepsilon s}(z_2)$ ($s = 1,2,3,4$) in volumetric lattice $N_1 \times N_2 \times N_3 = 30 \times 40 \times 67$ were obtained by the method of iterations on an index m for the four branches of the dimensionless complex displacement function by the formulas in [17, 20], respectively

$$u(z) = u_{\varepsilon 1}(z) = (g_1 - g_2 + g_4)/2; \quad u(z) = u_{\varepsilon 2}(z) = (g_1 - g_2 - g_4)/2;$$
$$u(z) = u_{\varepsilon 3}(z) = (-g_1 - g_2 + g_5)/2; \quad u(z) = u_{\varepsilon 4}(z) = (-g_1 - g_2 - g_5)/2. \quad (8)$$

Functions g_1, g_2, g_3, g_4, g_5 by analogy with [17, 20] are modeled by expressions

$$g_1(u,\alpha) = (1-\alpha)(1 - 2\,\mathrm{sn}^2(u - u_0, k))/Q; \quad (9)$$

$$g_2(z,\alpha) = 2^{-2\alpha} 3^{3\alpha - 1/2} \,|\, z - z_c \,|^{-\alpha}\, \Gamma(\alpha + 1/3)\Gamma(\alpha + 2/3)/\sqrt{\pi}\,\Gamma(\alpha + 1/2); \quad (10)$$

$$g_3(z,\alpha) = 3^{3\alpha - 1/2}\, 2|\, z - z_c \,|^{-2\alpha}\, \Gamma(\alpha + 1/3)\Gamma(\alpha + 2/3)/\pi;$$
$$g_4 = [(g_1 + g_2)^2 - g_3]^{1/2}; \quad g_5 = [(-g_1 + g_2)^2 - g_3]^{1/2}; \quad (11)$$

The initial expression for Q has the form

$$Q = p_0' + p_1' n + p_2' m + p_3' j - b_1\left(\frac{n' - n_0}{n_c}\right)^2 - b_2\left(\frac{m' - m_0}{m_c}\right)^2 - b_3\left(\frac{j' - j_0}{j_c}\right)^2. \quad (12)$$

The expression (12) has thirteen parameters. The parameter p_0' is independent of the variables n, m, j; parameters p_1', p_2', p_3' are included in the linear form; parameters b_1, b_2, b_3, n_0, n_c, m_0, m_c, j_0, j_c determine the behavior of the quadratic form. Parameters n_c, m_c, j_c play the role of semi-axes of fractal volumetric structures in a new coordinate system $O'n'm'j'$. The original coordinate system $Onmj$ is described in terms of variables n, m, j.

Performing spatial axis rotation of the coordinate system around axis Oj, we move from the system $Onmj$ to the system $O'n'm'j'$ by the formulas

$$n' = n \cdot k_1' \,\mathrm{cn}(u_{1\beta}, k_1) - m \cdot \mathrm{sn}(u_{1\beta}, k_1) + j \cdot k_1 \,\mathrm{cn}(u_{1\beta}, k_1);$$
$$m' = n \cdot k_1' \,\mathrm{sn}(u_{1\beta}, k_1) + m \cdot \mathrm{cn}(u_{1\beta}, k_1) + j \cdot k_1 \,\mathrm{sn}(u_{1\beta}, k_1);$$
$$j' = -n \cdot k_1 + j \cdot k_1'; \; k_1 = \mathrm{sn}(u_{1\theta}, k_{1\theta}); \; k_1' = \mathrm{cn}(u_{1\theta}, k_{1\theta}); \; k_1^2 + k_1'^2 = 1. \quad (13)$$

Here the dimensionless displacement $u_{1\beta}$ is connected with the polar angle $\varphi_{1\beta}$ in the plane Onm by relation $u_{1\beta} = F(\varphi_{1\beta}, k_1)$; F is an incomplete elliptic integral of the first kind; the dimensionless displacement $u_{1\theta}$ is connected with the effective angle θ_1 by relation $u_{1\theta} = F(\theta_1, k_{1\theta})$; $k_1, k_{1\theta}$ are modules of elliptic functions. The dimensionless displacement $u_{1\beta}$ is a

nonlinear function of two parameters $\varphi_{1\beta}$ and k_1, that define the different mechanisms of alteration of fractal volumetric structure and governing it. Here the parameter k_1 is a nonlinear function of $u_{1\theta}$ and $k_{1\theta}$. As a result, the displacement $u_{1\beta}$ becomes a complex function depending on three parameters $\varphi_{1\beta}$, $u_{1\theta}$, $k_{1\theta}$.In the calculations it should be: $z_1 = 0.053 + h_z(j_z + 33)$; $z_2 = 6.653 - h_z(j_z + 33)$; $h_z = 0.1$, which corresponds to the forward and backward waves of displacements $u_{nm}(z_1)$, $u_{nm}(z_2)$; $n = \overline{1,30}$; $m = \overline{1,40}$. For $j_z = 0$ we have $z_1 = z_2 = 3.353$.

Averaged functions $M_{\varepsilon s}$ have the form [15, 16, 20]

$$M = M_{\varepsilon s}(j) = Sp(\hat{\rho}_1 \hat{u}_{\varepsilon s}) = M'_{\varepsilon s} + iM''_{\varepsilon s}; \quad \hat{\rho}_1 = \hat{\xi}^T_{N2}\hat{\xi}_{N1} / N_2 N_1. \quad (14)$$

Here Sp is an operation of calculating the trace of a square matrix; «T» denotes transposition; $\hat{\xi}_{N1}$, $\hat{\xi}_{N2}$ are row-vectors with elements equal to one; $M'_{\varepsilon s} = \mathrm{Re}(M_{\varepsilon s})$, $M''_{\varepsilon s} = \mathrm{Im}(M_{\varepsilon s})$.

3. Stochastic state of the multilayer nanosystem

For the investigation of transient processes in multilayer nanosistem with nonlinear fractal oscillator the initial parameters were as follows: $k = 0.5$; $u_0 = 29.537$; $n_0 = 14.3267$; $n_c = 9.4793$; $m_0 = 19.1471$; $m_c = 14.7295$; $j_0 = 31.5279$; $j_c = 11.8247$; $p'_1 = 0$; $p'_2 = 0$; $p'_3 = 0$. In modeling the stochastic state deformation field of volumetric lattice it was assumed: $p'_0 = 1.0123$; $b_1 = b_2 = b_3 = 0$. For a negative fractal index $\alpha = -0.5$ the behavior of four branches (8) of displacement function u for forward and backward waves is given in Fig. 1, 2. These results were obtained for variant with $u_{1\beta} = 0$; $u_{1\theta} = 0$; $k_{1\theta} = 0$. From (14) it follows that the spatial rotation of the coordinate system is missing: $n' = n$; $m' = m$; $j' = j$. It was also assumed that $j_z = j'$, therefore, the displacement function $u(z) = u(z(j, j_z)) = u(z(j, j')) = = u(z(j, j)) = w(j)$ becomes a function on j. Note that the imaginary part of the displacement u is zero for all four branches, which indicates the anomalous behavior of the inverse structural states (with negative indices $\alpha \in (-2/3; -1/3)$) of the deformation field. When $j = 5$ for the forward wave (Fig. 1a,b,c) the behavior of displacement function for all branches is regular: along the axis Om for branches 3, 4 oscillations are observed; for branches 1, 2 the output on constant values with increasing m is characteristic (Fig. 1c). For the backward wave (Fig. 1d,e,f) besides regular behavior of branches 1, 2, 3 the pronounced stochastic behavior of branch 4 is observed. Note that for backward wave parameter $|z_2 - z_c|$ from the expression (10), (11) has a minimum for $j = 5$, and the parameter $|z_1 - z_c|$ changes monotonically on j. Behavior projection displacement u as functions of m for various j of the backward

wave (Fig. 2) clearly demonstrates the presence and features of transient processes (such as of structural alteration) in the model multilayer nanosystem. When $j_z = j' = j = 0$ (Fig. 2a) the displacement function for all branches of the backward and forward waves coincide. With increasing j the behavior of branches for the forward and backward waves begins to differ (Fig. 1).

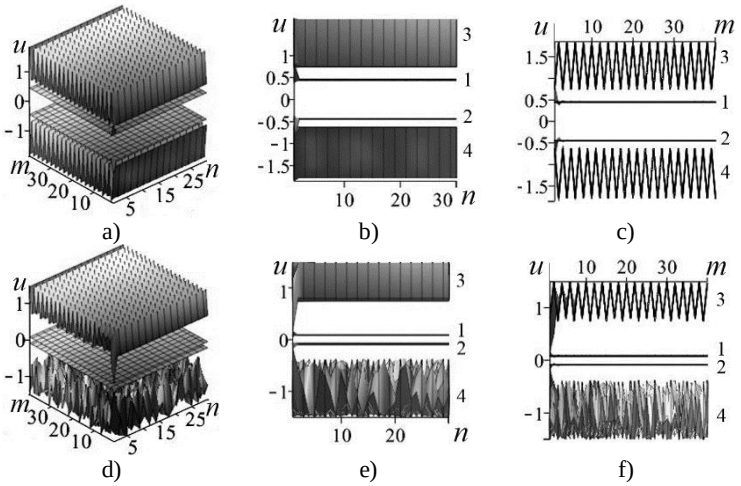

Fig. 1. Dependencies of the displacement function u and projections on planes nOu, mOu for forward (a, b, c) and backward (d, e, f) waves on the lattice indexes n, m: 1 – branch $u_{\varepsilon 1}$, 2 – branch $u_{\varepsilon 2}$, 3 – branch $u_{\varepsilon 3}$, 4 – branch $u_{\varepsilon 4}$; $j = 5$, $\alpha = -0.5$.

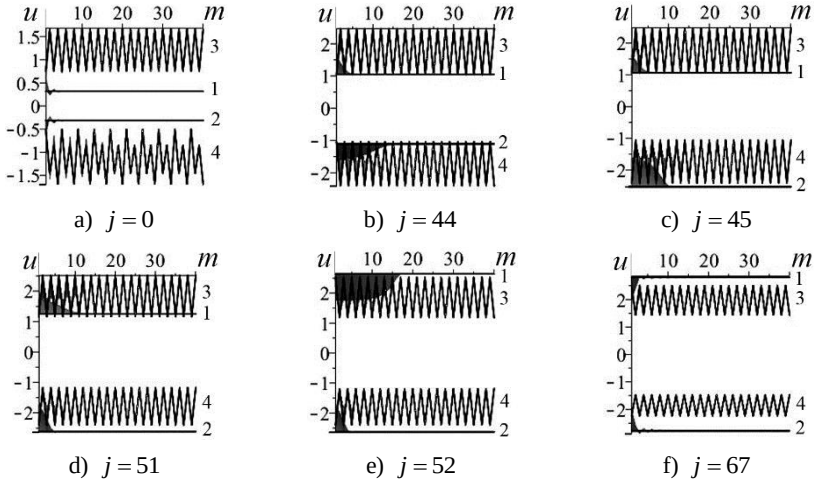

Fig. 2. Dependencies of the projections on plane mOu function u on m for different j: 1 – branch $u_{\varepsilon 1}$, 2 – branch $u_{\varepsilon 2}$, 3 – branch $u_{\varepsilon 3}$, 4 – branch $u_{\varepsilon 4}$; $\alpha = -0.5$, backward wave.

For backward wave the change of order of the branches is characteristic: for $j = 44$ (Fig. 2b) branch 2 is located above branch 4 and for $j = 45$ (Fig. 2c) branch 2 becomes below branch 4; for $j = 51$ (Fig. 2d) branch 1 is located below branch 3 and for $j = 52$ (Fig. 2e) branch 1 becomes above branch 3. This behavior is confirmed by the intersection of the dependence of the average functions M for backward wave (Fig. 3b). For forward wave the crossing effect and the changing of location order branches of the displacement function for values $j = 33$, $j = 34$ and $j = 41$, $j = 42$ are confirmed by the dependencies of the average functions M (Fig. 3a).

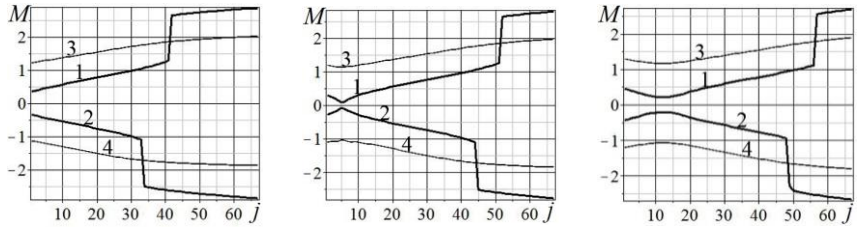

Fig. 3. Dependencies of functions M on j for four branches of displacement function u for forward (a) and backward (b) waves: curves 1, 2 (thick lines) - $M_{\varepsilon 1}$, $M_{\varepsilon 2}$; curves 3, 4 (thin lines) - $M_{\varepsilon 3}$, $M_{\varepsilon 4}$, respectively, $\alpha = -0.5$. Effect of rotation, backward wave (c).

On the dependencies of the average functions $M_{\varepsilon 1}$, $M_{\varepsilon 2}$ for forward and backward waves (Fig. 3a,b) there are features such as "inclined steps" that is characteristic of the hysteresis phenomena. For backward wave on the curves $M_{\varepsilon 1}$, $M_{\varepsilon 2}$, (Fig. 3b) for $j = 5$ the local minimum, maximum are also observed, respectively, which is typical for the type of behavior of the soft mode [20]. By choosing the parameters $u_{1\theta} = \pi / 8$, $k_{1\theta} = 1$, $u_{1\beta} = 0$ the rotation of the coordinate system is carried out. The influence of this rotation on the behavior of the averaged functions $M(j)$ for backward wave is given in Fig. 3c. Effects of shifting and broadening of the main features in comparison with Fig. 3b are observed. For values of the fractal index $\alpha \in (-1; -2/3)$ and $\alpha \in (-1/3; 1)$ all branches are characterized by the presence of both real and imaginary parts of the displacement function. For backward wave for $\alpha = 0.5$ the dependencies of the average complex functions are shown in Fig. 4. These results were obtained for the variant with parameters $u_{1\beta} = 0$; $u_{1\theta} = 0$; $k_{1\theta} = 0$ (excluding the effect of rotation). For all branches the presence of their critical value $j = j_k$ is characteristic. Within the regions of changes $j \in [1; j_k]$ the behavior of functions is stochastic. On the dependencies $M'_{\varepsilon s}$, $M''_{\varepsilon s}$ of the dimensionless time $j_z = j' = j$ transient processes with the formation of complex

shapes signals are observed, which allow the interpretation of the type of fractal induction, nutation, supernutation, echo, avalanches, self-induced transparency [7].

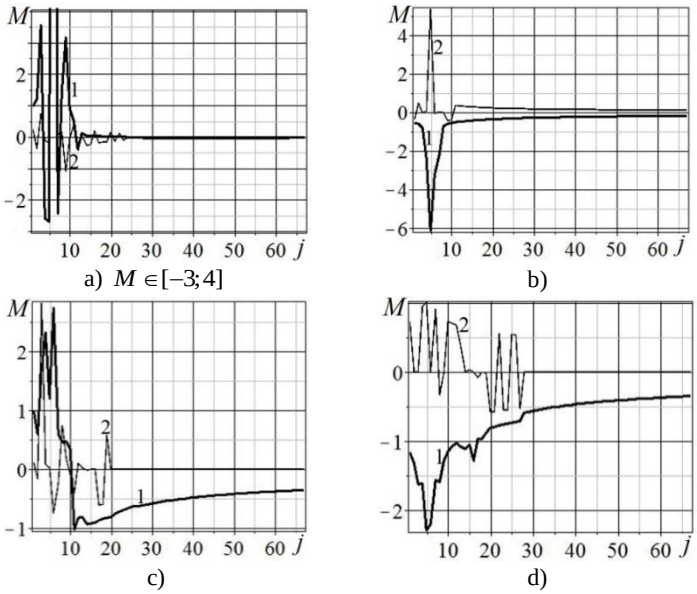

Fig. 4. Dependencies of M on j for four branches of u : a) $M_{\varepsilon 1} \in [-3;5]$; b) $M_{\varepsilon 2}$; c) $M_{\varepsilon 3}$; d) $M_{\varepsilon 4}$. Curve 1 (thick lines) - $M'_{\varepsilon s}$, curve 2 (thin lines) - $M''_{\varepsilon s}$; $\alpha = 0.5$, backward wave.

When $j > j_k$ the behavior of functions $M'_{\varepsilon s}(j)$, $M''_{\varepsilon s}(j)$ is almost regular with monotonic changes in the laws, close to power dependences. Note that the strongest changes of the averaged functions $M'_{\varepsilon s}(j)$, $M''_{\varepsilon s}(j)$ are observed near $j = 5$. At the same value j for inverse states with $\alpha = -0.5$ (Fig. 3) the behavior of the soft mode type is observed [20].

4. Quantum dot in multilayer nanosystem

For quantum dot the basic parameters were as follows: $p'_0 = -3.457 \cdot 10^{-11}$; $b_1 = b_2 = b_3 = 1$. Other parameters were the same as for the stochastic state. The choice of parameters corresponds to the location of the singular points of the deformation field on the fractal imaginary ellipsoid. First, we consider the state of a quantum dot with a fractal negative index $\alpha = -0.5$. On Fig. 5 there is an example of the behavior of the averaged functions M for the four branches (8) of forward (Fig. 5a) and backward (Fig. 5b) waves. These results have been obtained for the variant with $u_{1\beta} = 0$; $u_{1\theta} = 0$; $k_{1\theta} = 0$. On the dependencies $M_{\varepsilon 3}(j)$, $M_{\varepsilon 4}(j)$ of the forward and backward waves (Fig. 5a,b) such features as

"blurry steps" are observed compared with features such as "inclined steps" on the curves $M_{\varepsilon 1}(j)$, $M_{\varepsilon 2}(j)$ from Fig. 3a,b. On the dependencies $M_{\varepsilon 1}(j)$, $M_{\varepsilon 2}(j)$ (Fig. 5a,b) peak up, peak down for $j = 31$ appear, respectively. For backward wave for $j = 5$ at all four branches (Fig. 5b) local minima, maxima are additionally observed, which is typical for the behavior of the soft mode type [20].

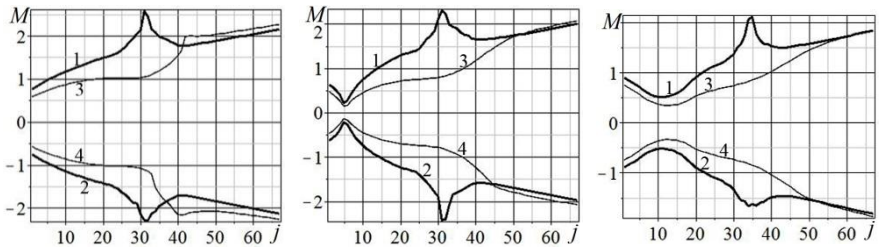

Fig. 5. Dependencies of M on j for four branches of u for forward (a) and backward (b) waves, $\alpha = -0.5$: curves 1, 2 (thick lines) - $M_{\varepsilon 1}$, $M_{\varepsilon 2}$; curves 3, 4 (thin lines) - $M_{\varepsilon 3}$, $M_{\varepsilon 4}$; effect of rotation for backward wave (c).

Between branches 1 and 3, 4 and 2 there is crossing of branches (Fig. 5a,b). By choosing the parameters $u_{1\theta} = \pi/8$, $k_{1\theta} = 1$, $u_{1\beta} = 0$ the rotation of the coordinate system is carried out. The influence of this rotation on the behavior of the averaged functions $M(j)$ for backward wave is given in Fig. 5c. The effects of shifting and broadening of the main features in comparison with Fig. 5b are observed. Below the behavior of the four branches (8) of displacement function u of forward wave for the characteristic values $j = 31$ (Fig. 6) and $j = 42$ (Fig. 7) is given. The imaginary part of the displacement function u for all branches is zero. For branch 1 (Fig. 6a) the presence of peak up localized near node (n_0, m_0) with a large amplitude and stochastic behavior in the quantum dot region (Fig. 6b) is characteristic. For branch 2 (Fig. 6c) a peak down is observed, which is also localized near the node (n_0, m_0) with other amplitude and stochastic behavior in the quantum dot region. For branch 3 (Fig. 6d) almost regular behavior with small positive amplitudes and minimum near the node (n_0, m_0) is observed. For branch 4 (Fig. 6e) almost regular behavior with small negative amplitudes and maximum near the node (n_0, m_0) is observed. On Fig. 6f the section $u \in [-2; 2]$ of all four branches together is given: branches 1 and 3 generally have positive values, 2 and 4 – negative. There is the crossing of the four branches of the displacement function at separate points. Between the branches of the displacement function gaps are observed. With an increase of j the behavior of all four branches of the displacement function changes (Fig. 7). This is due to the change $Q(j)$ (13) and

the parameter $|z(j)-z_c|$ from expressions (10), (11) for four branches of the displacement function (8). The changes in the values of gaps between the branches of displacement function are also observed. Note that the behavior of the four branches of the displacement function, the gaps between the branches, the location of the singular points are qualitatively similar to the behavior of the physical parameters close to the Dirac points [2, 3]. It is also possible to have the physical interpretation of the displacement function as a function of the dimensionless wave number $q_z=(z-z_c)/z_c$.

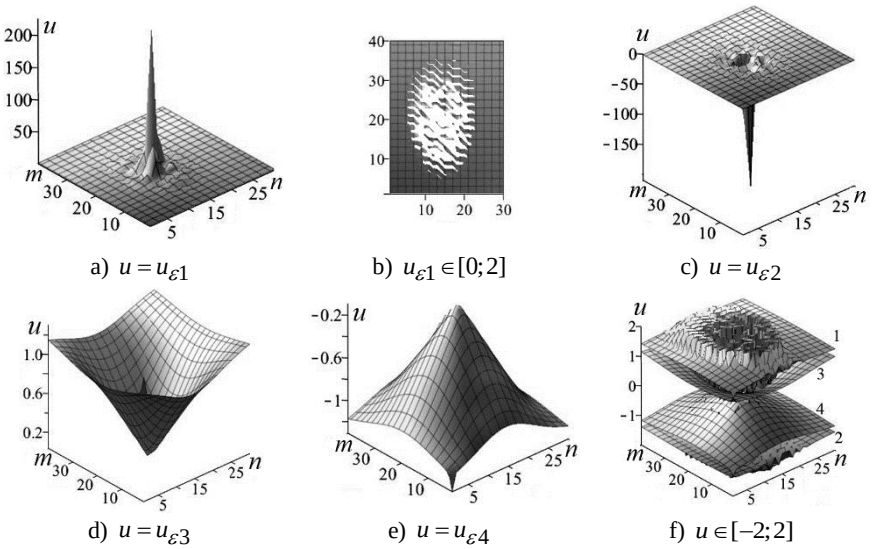

Fig. 6. Dependencies of u on the lattice indexes n, m for forward wave: (a) 1 – branch $u_{\varepsilon 1}$, (b) cut $u_{\varepsilon 1}\in[0;2]$ (top view), (c) 2 – branch $u_{\varepsilon 2}$, (d) 3 – branch $u_{\varepsilon 3}$, (e) 4 – branch $u_{\varepsilon 4}$, (f) dependences of the four branches; $j=31$, $\alpha=-0.5$.

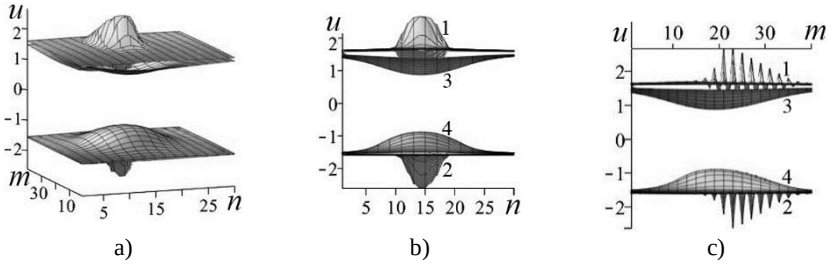

Fig. 7. Dependencies of u (a), the projections on planes nOu (b) and mOu (c) on the lattice indexes n, m for forward wave: 1 – branch $u_{\varepsilon 1}$, 2 – branch $u_{\varepsilon 2}$, 3 – branch $u_{\varepsilon 3}$, 4 – branch $u_{\varepsilon 4}$; $j=42$, $\alpha=-0.5$.

When $\alpha = 0.5$ the displacement function u is complex. Each of the functions $M'_{\varepsilon s}$, $M''_{\varepsilon s}$ (Fig. 8) has the characteristic range of values $j \in (j_0 - j_{ks}; j_0 + j_{ks})$, within the behavior of these functions are very different. Here j_{ks} is some critical value.

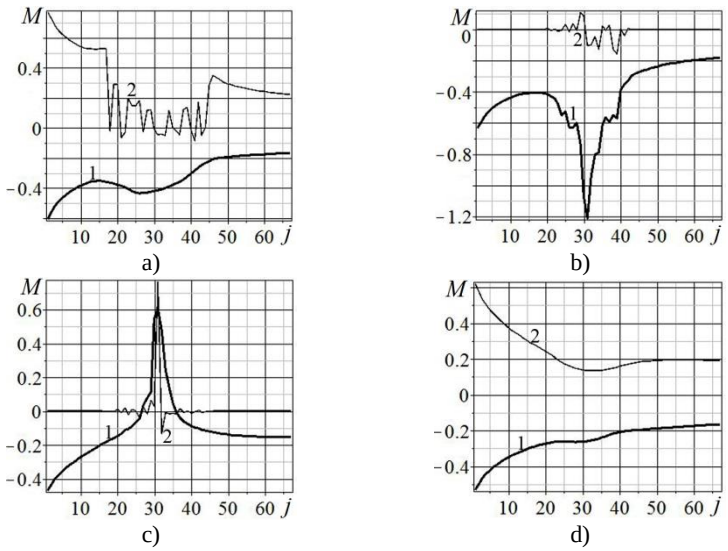

Fig. 8. Dependencies of M on j for four branches of u : a) $M_{\varepsilon 1}$; b) $M_{\varepsilon 2}$; c) $M_{\varepsilon 3}$; d) $M_{\varepsilon 4}$. Curve 1 (thick lines) - $M'_{\varepsilon s}$, curve 2 (thin lines) - $M''_{\varepsilon s}$; $\alpha = 0.5$, forward wave.

So functions $M''_{\varepsilon 1}$, $M''_{\varepsilon 2}$, $M''_{\varepsilon 3}$ within specific intervals have pronounced stochastic behavior, and the behavior of functions $M'_{\varepsilon 1}$, $M'_{\varepsilon 3}$, $M'_{\varepsilon 4}$, $M''_{\varepsilon 4}$ is almost regular. Function $M'_{\varepsilon 2}$ describes the formation of a signal with a complex shape. On dependencies $M'_{\varepsilon 2}$, $M'_{\varepsilon 3}$, $M''_{\varepsilon 2}$ near the value j_0 pronounced peaks are observed. The behavior of the functions (Fig. 8) demonstrates the possibility of the appearance of various transient processes in a model multilayer nanosystem with quantum dot. The analysis of these dependencies allows us to estimate the critical values j_{ks}, that are associated with the dimensionless relaxation times of each of the branches $u_{\varepsilon s}$ of the complex displacement function u. Outside characteristic intervals all functions practically change monotonous by its laws.

5. Conclusions

The behavior of the four branches of the complex displacement function on the dimensionless time for the stochastic state and the fractal quantum dot in model multilayer nanosystem is investigated. The appearance of four branches is connected with the bifurcation effect of solutions of nonlinear equations system for multilayer nanosystem with fractal oscillator. For values of the fractal index $\alpha \in (-1; -2/3)$ and $\alpha \in (-1/3; 1)$ all branches are characterized by the presence

of both real and imaginary parts of the displacement function. It is shown that changing the dimensionless time may cause transient effects such as fractal induction, nutation, supernutation, echo, avalanches, self-induced transparency. Within the range of variation of the fractal index $\alpha \in (-2/3; -1/3)$ the imaginary part of displacement function is zero for all four branches, which indicates the anomalous behavior of the inverse structural states. The analysis of the behavior of the averaged functions and displacement functions allows to reveal features such as soft mode, "inclined steps", the presence of hysteresis, gaps between the branches of displacement function, the presence type of singular Dirac points. By increasing the dimensionless time the change of the structure of the displacement field of each of the four branches, the change of the gaps between the branches, the crossing of the branches in selected areas (transient processes type of structural alteration) take place.

References

1. M.O. Scully, M.S. Zubairy. *Quantum Optics.* Cambridge: Cambridge Univ. Press, 1997.
2. L. Tarruell, D. Greif, T. Uehlinger et. all. Greating, moving and merging Dirac points with a Fermi gas in a tunable honeycomb lattice. *Nature* **483,** 7389: 302-305, 2012.
3. K.K. Gomes, W. Mar, W. Ko et. al. Designer Dirac fermions and topological phases in molecular graphene. *Nature* **483,** 7389: 306-310, 2012.
4. M. Warner, S. Din, I. Tupitsyn et. al. Potential for spin-based information processing in a thin-film molecular semiconductor. *Nature* **503,** 7477: 504-508, 2013.
5. L. Allen, J.H. Eberly. *Optical Resonance and Two-level Atoms.* Wiley Interscience Publication, New York-London-Sydney-Toronto, 1975.
6. M.V. Chekhova, M.V. Fedorov. The Schmidt modes of biphoton qutrits: Poincare-sphere representation. *J. Phys. B: At. Mol. Opt. Phys.*, 46(095502): 1-10, 2013.
7. S. Alexander, O. Entin-Wohlman, R. Orbach. Relaxation and nonradiative decay in disordered systems. I. One-fracton emission. *Phys. Rev. B.* **32,** 10: 6447-6455, 1985.
8. V.S. Abramov. Fractal induction, avalanche, self-induced transparency, the echo in the model nanosystem. Materials of the X International Symposium on photon echo and coherent spectroscopy (PECS'2013). Yoshkar-Ola: FSBEI HPO: 78-86, 2013.
9. J. Balewski, A. Krupp, A. Gaj et. al. Coupling a single electron to a Bose-Einstein condensate. *Nature* **502,** 7473: 664-667, 2013.
10. H.-J. Stockmann. *Quantum Chaos. An Introduction.* Cambridge Univers. Press, 1999.
11. Jan Awrejcewicz, V.A. Krysko. *Chaos in Structural Mechanics*. Springer-Verlag Berlin Heidelberg, 2008.
12. C.H. Skiadas, C. Skiadas. *Chaotic Modeling and Simulation: Analysis of Chaotic Models, Attractors and Forms.* Taylor and Francis/CRC, London, 2009.
13. M.V. Zakrzhevsky, R.S. Smirnova, I.T. Schukin, et all. *Nonlinear dynamics and chaos. Bifurcation groups and rare attractors*. Riga, RTU, Publishing House, 2012.
14. O.P. Abramova, S.V Abramov. Fractal nanotraps based on quasi-two-dimensional fractal structures. *Dynamical Systems Theory* (Editors J.Awrejcewicz et. al.) DSTA 2013, Lodz, December 2-5, Poland: 71-80, 2013.
15. V.S. Abramov. Fractal dislocation as one of non-classical structural objects in the nano-dimensional systems. *Metallofiz. i Noveishie Tekhnologii*. **33,** 2: 247-251, 2011.
16. V.S. Abramov. Correlation Relations and Statistical Properties of the Deformation Field of Fractal Dislocation in a Model Nanosystem. *Chaotic Modeling and Simulation (CMSIM) Journal.* **3**: 357-365, 2013.

17. V.S. Abramov. Behavior of the deformation field of fractal dislocation in the presence of bifurcftions. *Bul. of Donetsk Nat. Univers.* **Ser. A,** 2: 23-29, 2011.
18. V.S. Abramov. Features of statistical properties of the deformation field of the fractal dislocation. *Bul. of Donetsk Nat. Univers*. **Ser. A,** 1: 105-113, 2012.
19. O.P. Abramova, S.V Abramov. Governance of Alteration of the Deformation Field of Fractal Quasi-two-dimensional Structures in Nanosystems. *Chaotic Modeling and Simulation (CMSIM) Journal*. **3**: 367-375, 2013.
20. V.S. Abramov. Inverse structural states of the stochastic deformation field of fractal dislocation. *Fizika i Tekhnika Vusokikh Davleniy*. **23**, 3: 54-62, 2013.